

²³⁰TH/U DATING OF THE TROJAN ‘WATER QUARRIES’*

N. FRANK† and A. MANGINI

*Heidelberger Akademie der Wissenschaften, Forschungsstelle Radiometrie,
Im Neuenheimerfeld 229, D-69120 Heidelberg, Germany*

and M. KORFMANN

*Institut für Ur- und Frühgeschichte und Archäologie des Mittelalters, Universität,
Schloss, D-72070 Tübingen, Germany*

We determined the ²³⁰Th/U ages of individual calcite layers that grew on the walls of artificial water-supply tunnels (‘water quarries’) at Troy/Ilios by using thermal ionization mass spectrometry. The oldest age of overgrowth being 4350 ± 570 years, the tunnels must have been built a short time earlier, during the archaeological period Troy I–II. The tunnels were also used during Troy VI–VII (1700–1150 BCE, a period that includes the date of the supposed ‘Trojan War’), in Homeric times (c. 720 BCE) and in the Roman period. These findings add strong support to the identification of the water quarries with a natural phenomenon and Anatolian deity known in Hittite texts of the second millennium BCE as KASKAL.KUR, a term denoting subsurface water systems. Consequently, they reinforce the view that Troy in the second millennium BCE was Anatolian in character. In this way, the findings are also consistent with the identification of (W)Ilios with Wilusa, a city attested to in Hittite historical texts.

KEYWORDS: U-SERIES DATING, TROY/ILIOS, KASKAL.KUR, ANATOLIA

INTRODUCTION

The site of Troy exhibits a complex evolution, the interpretation of which poses many puzzles. Situated on the sea coast, it was influenced in its early stages, during the Bronze Age (Troy I–VII), by Anatolian and southeastern European cultures; in later stages it was influenced by Greek, Roman and Byzantine cultures. Recent research and excavation, however, clearly point to the conclusion that during the Troy VI–VIIa period (c. 1700–1150 BCE) the site had a culture that was principally oriented towards Anatolia (Korfmann 1994, 1996, 1998a, 2000). This is the period of the ‘Trojan High Culture’, the end of which is supposed by some to have coincided with the ‘Trojan War’, which may have formed the backdrop to events described by Homer in the Iliad (c. 720 BCE).

In the second millennium BCE the name of the city was probably Wilusa/Taruisa [= (W)Ilios/Troia] (Starke 1997). This identification has an important consequence. A treaty of c. 1280 BCE between the Luwian king Alaksandu of Wilusa and the Hittite king Muwatallis of Hatusa refers to a god of Wilusa named KASKAL.KUR. The term denotes a subsurface water system: KASKAL = ‘path’ or ‘tunnel’, KUR = ‘underworld’ or ‘underground’; and the system was

* Received 9 July 2001; accepted 9 November 2001.

† Present address: Laboratoire des Sciences du Climat et de l’Environnement, CNRS, Bât. 12, 3 Avenue de la Terrasse, 91198 Gif-sur-Yvette, France.

© University of Oxford, 2002

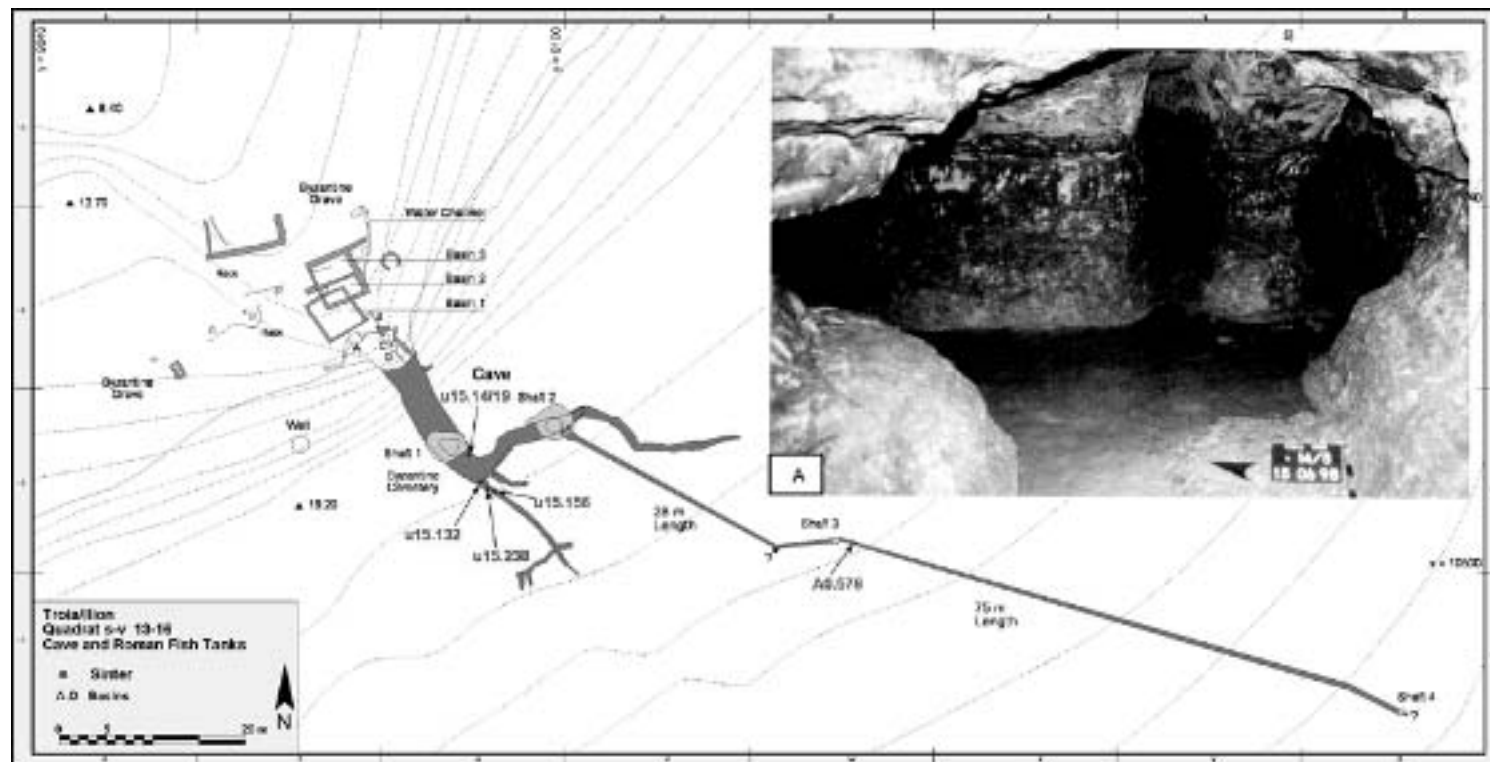


Figure 1 A schematic map and cross-section image of the 'water quarries' at Troy. The black area reflects the tunnel system excavated during 1997–9. The dark grey area represents the gallery that was explored in the year 2000. The water quarries are located on the northwestern flank of the ancient lower city of Troy, where the slope of the hill is steep (dotted lines indicate the topography). Three Roman basins and at least four pre-Roman wash-basins have been excavated in front of the main entrance to the tunnel system. These rock-cut early basins were connected to the water channel, which runs through the tunnels. So far, four shafts have been found connecting the water system with the hill surface. Carbonate samples were collected at several sites within the tunnel system.

sufficiently important to the city of Wilusa to be regarded as a deity. Such a water system could therefore have existed at Ilios/Troia in the Troy VI–VIIa period (Korfmann 1998b). It was possible that, if such a feature could be found, it would also provide the answer to a long-debated problem of Homeric topography: the possible location of the springs which, according to the Iliad (XVII, 147–56), Achilles and Hector passed during their final combat. Such springs could have been visible in Homer's own days (c. 720 BCE), if we assume that Homer provides a relatively accurate geographical picture of the locality during his own time. This says nothing, however, about the historical aspects of the Iliad, which are the subject of other disciplines.

During 1997–2000, the excavation of a system of artificially constructed water supply tunnels was resumed and extended (Korfmann 1998b, 1999, 2000). To the present stage of excavation, the tunnels extend over more than 100 m and the diameter varies in size (Fig. 1).

At the entrance near the excavated water basins, the tunnels are between 4 and 6 m wide, but within the deeper part there are only narrow tubes of ~1.5–0.8 m size. So far, four shafts have been found connecting the water quarries with the surface of the hill; in other words, the ancient city. Roman use was well attested archaeologically, but it was uncertain whether the tunnels had been built at some earlier date. The walls of the tunnels are in parts overgrown with calcite, up to 4 cm thick. These accretions have been deposited by water-bearing elevated CO_2 concentrations.

Secondary carbonates, such as stalagmites and flowstones, can be accurately dated by thermal ionization mass spectrometric $^{230}\text{Th}/\text{U}$ techniques. Due to further developments of this technique, it is possible to determine precise and accurate ages well within the ^{14}C time scale (Baker *et al.* 1993; Burns *et al.* 1998; Frumkin *et al.* 1999; Williams *et al.* 1999; Neff *et al.* 2001). The accuracy of $^{230}\text{Th}/\text{U}$ chronologies of carbonates requires a closed-system behaviour for the gain and loss of U and Th, negligible or even ^{232}Th -correctable abundance of ^{230}Th , ^{234}U and ^{238}U from detritus, and negligible initial ^{230}Th (Kaufmann and Broecker 1965; Ludwig and Titterton 1994; Frank *et al.* 2000). Here, we selected pure calcite layers for $^{230}\text{Th}/\text{U}$ dating having minor detrital contamination and showing no visible sign of alteration. By doing so, we were able to reconstruct the chronology of the calcite overgrowth (flowstone) at five sites within the tunnel system.

SAMPLES AND METHODS

Figure 2 shows slabs of the flowstones that have been taken from the tunnel walls during the past three years of excavation. Carbonate was often precipitated directly on the tunnel walls and thus mirrors the extremely uneven structure of the surface. In one case (sample AO576), calcite was precipitated on limestone-rich sediments within a part of the gallery far apart from the entrance area. Calcite layers that are oriented towards the tunnels walls (the topmost 0.5 cm) reflect a highly porous texture with irregular banding. The dark yellow to red colour originates from homogeneously distributed detrital particles, such as clay and silt. Later on, the calcite layers became more and more laminar and detrital contamination strongly decreases. The outermost parts of these deposits reflect a clearly banded texture with a perfectly white colour. In two of the studied plates, we found small pieces of charcoal included into the laminar calcite fabric (pieces u15.14-19 and u15.132). The occurrence of fine ash particles within a cave environment where calcite is precipitated leads to a grey colour of the calcite layers, which is obviously the case within the outermost layers of piece u15.14-19 and within the centre part of piece u15.132. Hence, during the evolution of these calcite layers, any form of open fire was frequently used at the entrance area of the water quarries or in the tunnel itself.

From the slabs presented in Figure 2, we cut samples parallel to the growth axis (size ~0.3 cm^3) for $^{230}\text{Th}/\text{U}$ dating (arrowhead in Fig. 2). Samples from the detritus-rich parts of the

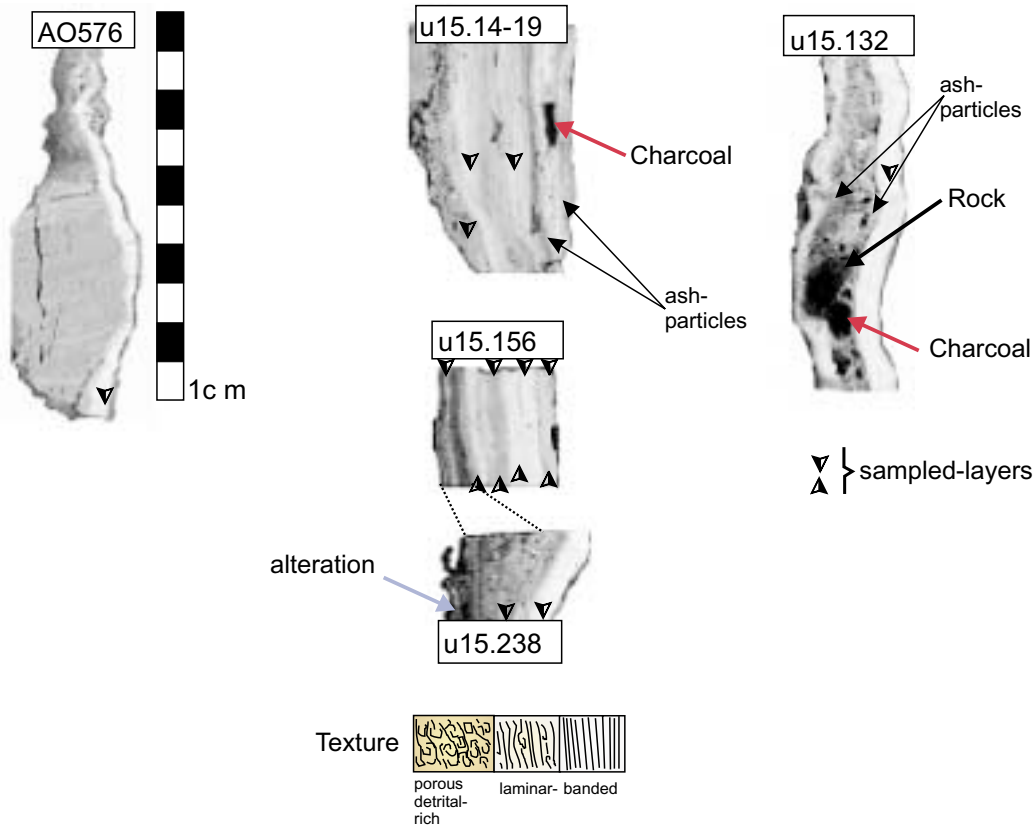


Figure 2 Cross-section images of the five investigated secondary calcite deposits of water-supply tunnels at Troy. We collected samples (arrowheads) by using a diamond-bladed band saw, which enabled us to cut off certain growth bands of different lithology and hence of different age.

deposits u15.238, u15.156 and u15.132 were not studied, as they do not meet the dating requirements mentioned above.

The samples were rinsed several times with quartz-distilled water and suprapure diluted nitric acid to remove surface contamination. The cleaned pieces were crushed and then dissolved with concentrated suprapure nitric acid. A defined quantity of a ^{229}Th spike and a $^{233}\text{U}/^{236}\text{U}$ double spike was added to determine the concentrations of ^{230}Th , ^{234}U , ^{238}U and ^{232}Th . Insoluble silicate components were centrifuged, dried and weighed to determine the average contamination with detritus. Chemical separation and purification of U and Th closely followed the procedure described by Ivanovich and Harmon (1992). Th and U isotopes were separated using iron for coprecipitation, purified utilizing DOWEX 1X8 resin in nitric form and placed on a preheated rhenium filament for mass spectrometric analyses. Chemical blanks yielded less than 0.2 ng of ^{238}U and 0.13 ng of ^{232}Th , respectively.

We measured the isotopic composition of both elements on a thermal ionization mass spectrometer (TIMS) (MAT 262 RPQ I/Finnigan Bremen), applying a double filament technique for both metals. Measurements of U were performed applying a semi-peak jump routine on the multicollector. U standard material NBL-112a (former National Brunswick Laboratories—later

on referred to as NBS-SRM960 and NIST4321B) yielded an average $^{234}\text{U}/^{238}\text{U}$ atomic ratio of $52.79 \times 10^{-6} \pm 2\%$ (2σ mean, $N = 23$), in good agreement with previously published values (Eisenhauer *et al.* 1992; Edwards *et al.* 1993; Bard *et al.* 1998; Sturchio *et al.* 1994; Frank *et al.* 2000).

Th isotopic analyses were performed with a peak jump routine. To determine the reproducibility of mass spectrometric Th and U isotope analyses, we repeatedly measured the isotopic composition of a ^{232}Th – ^{230}Th standard ($N = 15$) and of NBL-112a ($N = 23$). The external reproducibilities of the Th and U isotopic ratios are $\pm 0.6\%$ and $\pm 0.5\%$ respectively.

RESULTS AND DISCUSSION

Calcite layers at the water quarries of Troy exhibit a high but variable U concentration ranging from 2.28 to 0.71 $\mu\text{g g}^{-1}$ (Table 1). The U isotopic composition (Table 1) is given as ‰-offset from radioactive equilibrium—that is, $\delta^{234}\text{U} = (^{234}\text{U}/^{238}\text{U}_{\text{measured}}/^{234}\text{U}/^{238}\text{U}_{\text{equilibrium}} - 1) \times 1000$ —and shows an average value of +164‰, with a total range of +100 to +220‰. The U isotopic ratio and concentration variations do not correlate with each other. Thus, the pronounced concentration changes most probably reflect geochemical or physical changes during the depositional process, which does not affect the U isotopic composition. In contrast, variations of U sources to the drip water—that is, processes acting during U weathering from the host rock, or dissolution and re-crystallization of calcite layers—would influence the U isotopic composition (Ivanovich and Harmon 1992).

Detrital contamination of the studied samples is strictly coupled to the amount of the natural most abandoned Th isotope, ^{232}Th . All samples contained minor amounts of insoluble aluminosilicate minerals, which typically contain 6400–10 000 ng g^{-1} of ^{232}Th (tonalites and upper crust values from Wedepohl 1995). White laminar calcite has typically less than 1% detritus, which is leached during sample dissolution and yielded on average 10 ng g^{-1} of ^{232}Th .

The parts of the calcite overgrowth that have no laminar banding but a more porous texture, as shown in Figure 2, contain more variable amounts of insoluble residue ranging from 2% to 5% and have ^{232}Th concentrations of between ~50 and 120 ng g^{-1} . Detritus adds ^{230}Th as well as U isotopes to the calcite, which do not reflect the radioactive disequilibrium caused by calcite formation. Hence, a correction for detritus-derived ^{230}Th , ^{234}U and ^{238}U is necessary to determine accurate ages for the different layers. As a first order estimate, we assume that the detritus present in our sample reflects average ^{232}Th , ^{230}Th , ^{234}U and ^{238}U compositions that are similar to those of the average continental crust. In this case, the detrital $^{238}\text{U}/^{232}\text{Th}$ activity ratio is ~0.75 (the average of the mean continental crust and tonalites; Wedepohl 1995) and the U series nuclides are assumed to be in secular equilibrium. Hence we subtract the detrital ^{230}Th activity [^{230}Th]_{detritus}—that is, $0.75 \pm 0.1 \times ^{232}\text{Th}$ activity—from the measured ^{230}Th activity to obtain the corrected $^{230}\text{Th}_{\text{cor}}$ activity of the pure calcite:

$$[^{230}\text{Th}]_{\text{cor}} = [^{230}\text{Th}]_{\text{measured}} - 0.75 \times [^{232}\text{Th}]. \quad (1)$$

Similar equations can be deduced to correct the ^{238}U and ^{234}U activities.

This correction is significant but small for white laminar banded calcite layers, as it is on average 7% of the total measured ^{230}Th concentration. For U isotopes it is less than 0.5% and can be considered negligible within uncertainty of measurement. Some of the calcite layers close to the tunnel walls contain large amounts of detrital material, which strongly increases the total ^{230}Th activity of a sample and thus the uncorrected age of the calcite layer. The correction factor—that is, [^{230}Th]_{detritus}—can be as high as 29% of the measured ^{230}Th activity.

Table 1 *U and Th concentrations, $^{230}\text{Th}/^{238}\text{U}$ and $^{230}\text{Th}/^{232}\text{Th}$ activity ratios, and U isotopic ratios and ages*

| Sample | ^{238}U ($\mu\text{g g}^{-1}$) | ^{232}Th (ng g^{-1}) | $[^{230}\text{Th}/^{238}\text{U}]$ | $[^{230}\text{Th}/^{232}\text{Th}]$ | $\delta^{234}\text{U}_t$ (‰) | Age (10^3 a) | Age-corrected (10^3 a) |
|-----------------------------------|---|--|------------------------------------|-------------------------------------|------------------------------|-----------------|---------------------------|
| U15.14-19* | 2.221 | 94.6 | 0.0483 ± 0.0011 | 3.42 ± 0.07 | 169.2 ± 8.2 | 4.61 ± 0.13 | 3.61 ± 0.11 |
| U15.14-19 | 1.987 | 10.6 | 0.0273 ± 0.0007 | 15.44 ± 0.41 | 130.8 ± 7.5 | 2.68 ± 0.09 | 2.55 ± 0.09 |
| U15.14-19 | 1.865 | 10.9 | 0.0279 ± 0.0007 | 14.39 ± 0.34 | 132.5 ± 5.6 | 2.73 ± 0.08 | 2.59 ± 0.08 |
| AO576 | 1.585 | 10.2 | 0.0235 ± 0.0002 | 11.01 ± 0.09 | 181.5 ± 6.5 | 2.20 ± 0.03 | 2.06 ± 0.03 |
| U15.238* | 1.912 | 63.8 | 0.0374 ± 0.0006 | 3.38 ± 0.05 | 193.7 ± 6.5 | 3.49 ± 0.08 | 2.72 ± 0.06 |
| U15.132 | 1.634 | 2.9 | 0.0191 ± 0.0006 | 32.31 ± 0.98 | 182.2 ± 11.8 | 1.78 ± 0.07 | 1.74 ± 0.07 |
| U15.156-1* | 2.284 | 124.9 | 0.0585 ± 0.0016 | 3.22 ± 0.09 | 134.4 ± 8.0 | 5.78 ± 0.20 | 4.46 ± 0.16 |
| U15.156-2 | 0.711 | 11.3 | 0.0527 ± 0.0055 | 9.96 ± 1.0 | 192.3 ± 18.8 | 4.95 ± 0.60 | 4.59 ± 0.54 |
| U15.156-3* | 1.541 | 63.4 | 0.0523 ± 0.0027 | 3.83 ± 0.2 | 168.3 ± 6.1 | 5.00 ± 0.29 | 4.04 ± 0.24 |
| <i>Isochron of U15.156-1 to 3</i> | | | 0.0456 ± 0.0078 | — | 210.7 ± 4.5 | | 4.20 ± 0.75 |
| U15.156-4 | 0.767 | 9.5 | 0.0347 ± 0.0020 | 8.49 ± 0.48 | 101.9 ± 8.5 | 3.50 ± 0.23 | 3.20 ± 0.21 |
| U15.156-5 | 1.00 | 11.0 | 0.0326 ± 0.0047 | 8.90 ± 1.3 | 147.1 ± 16.6 | 3.16 ± 0.50 | 2.90 ± 0.46 |
| U15.156-6 | 1.710 | 19.9 | 0.0191 ± 0.0006 | 7.93 ± 0.17 | 221.6 ± 7.6 | 2.78 ± 0.08 | 2.52 ± 0.07 |
| U15.156-7 | 0.886 | 14.9 | 0.0255 ± 0.0012 | 4.58 ± 0.21 | 153.1 ± 6.1 | 2.45 ± 0.13 | 2.05 ± 0.11 |
| U15.156-8 | 1.704 | 18.0 | 0.0245 ± 0.0011 | 7.01 ± 0.31 | 174.6 ± 8.8 | 2.31 ± 0.12 | 2.06 ± 0.11 |

U isotopic analyses were carried out by using a newly mixed $^{236}\text{U}/^{233}\text{U}$ double spike. Its isotopic composition was adjusted to an atomic ratio of 118.5 ± 0.4 , close to the atomic ratio, of 132.14, of $^{235}\text{U}/^{234}\text{U}$ in secular equilibrium. We adjusted the amount of the U spike in such a way as to obtain atomic ratios of $^{234}\text{U}/^{233}\text{U}$ and $^{235}\text{U}/^{236}\text{U}$ close to 1, to avoid any potential problem caused by variable electron multiplier (EM) efficiency. We adopted the natural $^{238}\text{U}/^{235}\text{U}$ atomic ratio of 137.88 to determine the thermal fractionation, and used the $^{236}\text{U}/^{233}\text{U}$ ratio to correct for drifts of Faraday cup to electron multiplier calibration. The abundance sensitivity was determined prior to the analyses by performing a detailed mass scan over the range of masses 233.8–237.8. The influence of scatter ions from mass 238 was determined assuming a linear decline of scatter ions between mass 237.8 and 233.8 and amounts to average 2.5‰ of the signal on mass 234 over the course of our experiments. Th isotopic analyses were performed solely by using the second available electron multiplier, which is set behind the retarding potential quadrupole (RPQ). Abundance sensitivity corrections are negligible in this case. $^{232}\text{Th}/^{229}\text{Th}$ atomic ratios were determined before and after the detection of $^{230}\text{Th}/^{229}\text{Th}$ by using the first-stage electron multiplier to study thermal fractionation and to avoid high count rates on the second electron multiplier.

The activity ratios of $^{234}\text{U}/^{238}\text{U}$, $^{230}\text{Th}/^{238}\text{U}$ and $^{230}\text{Th}/^{232}\text{Th}$ were calculated from atomic ratios utilizing half-lives given by Cheng *et al.* (2000): $T_{1/2}(^{238}\text{U}) = 4.468 \cdot 10^9$ a, $T_{1/2}(^{234}\text{U}) = 245 \cdot 10^3$ a, $T_{1/2}(^{230}\text{Th}) = 75 \cdot 10^3$ a and $T_{1/2}(^{232}\text{Th}) = 1.401 \cdot 10^{10}$ a, respectively. Measured $^{234}\text{U}/^{238}\text{U}$ activity ratios are reported as $\delta^{234}\text{U}$ (‰) = $([^{234}\text{U}/^{238}\text{U}] - 1) \times 1000$. Uncertainties are given as 2σ error of mass spectrometric counting statistic.

Ages are iteratively determined from (a) measured $^{230}\text{Th}/^{238}\text{U}$ activity ratios and $\delta^{234}\text{U}$ and (b) ^{232}Th -corrected activity ratios (equation (1)), applying the following equation (Ivanovich and Harmon 1992):

$$\frac{^{230}\text{Th}}{^{238}\text{U}} = (1 - e^{-\lambda_{230}t}) + \frac{\lambda_{230}}{\lambda_{230} - \lambda_{234}} \left(\frac{\delta^{234}\text{U}}{1000} \right) (1 - e^{-(\lambda_{230} - \lambda_{234})t}).$$

* An asterisk marks samples that have a detritus content of more than 2% and less than 5%.

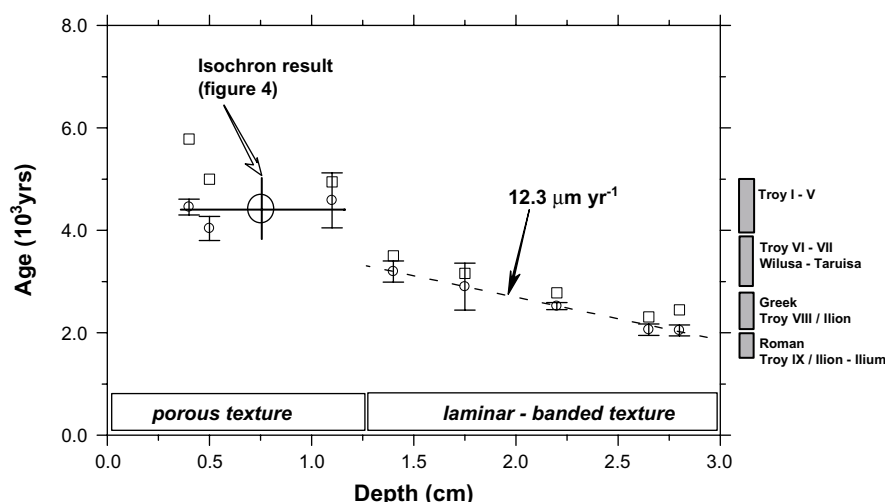


Figure 3 A plot of $^{230}\text{Th}/\text{U}$ ages and lithology versus depth of sample u15.156. Circles represent ages corrected for the influence of detritus following the model given in the text. Squares represent the ages without correcting for the influence of detritus. Calcite layers oriented towards the tunnel wall have a porous texture and exhibit no age differences, which indicates a fast growth rate. The following five investigated laminar-banded calcite layers indicate a smooth decrease of ages from 3000 to 2000 years (1000 to 0 years BCE). On the right-hand side of the plot, historical epochs are indicated.

Because these samples are most important to determine the timing of the tunnel construction, we carefully evaluated our simple correction model. On sample u15.156 we studied eight consecutive layers, which yield ^{232}Th -corrected $^{230}\text{Th}/\text{U}$ ages that systematically decrease from ~4200 years to about 2000 years (Fig. 3). However, the age correction is extremely high (–1000 years and –1300 years) for the oldest two samples, weakening any interpretation of the initiation of calcite overgrowth. Samples from the outermost 2 cm of this piece of calcite overgrowth exhibit a growth rate of $12.3 \mu\text{m a}^{-1}$, a value that agrees well with typical growth rates of cave deposits such as stalagmites and flowstones ranging from tens to hundreds of micrometres per year.

To study the detritus correction in more detail, Figures 4 (a) and (b) show plots of the activity ratios of $^{230}\text{Th}/^{232}\text{Th}$ versus $^{238}\text{U}/^{232}\text{Th}$ (Fig. 4 (a)) and $^{234}\text{U}/^{232}\text{Th}$ versus $^{238}\text{U}/^{232}\text{Th}$ (Fig. 4 (b)). These plot types are called Rosholt Type II isochrons and are used to determine ^{232}Th free activity ratios of $^{230}\text{Th}/^{238}\text{U}$ and $^{234}\text{U}/^{238}\text{U}$ (Ludwig and Titterton 1994, and references therein). For a set of calcite samples of equal age having different detrital contamination—that is, different ^{232}Th activities—one would obtain a straight mixing line. The slope of this mixing line gives the ^{232}Th free activity ratios of $^{230}\text{Th}/^{238}\text{U}$ and $^{234}\text{U}/^{238}\text{U}$ used for $^{230}\text{Th}/\text{U}$ dating (Ludwig and Titterton 1994). In our case the different calcite layers are not expected to be cogenetic and thus should not define a linear mixing line. In contrast to this assumption, the three samples taken from the part of the calcite overgrowth that has a porous texture nicely represent a mixing line, while the others do not. The data points below this line indicate a younger age, in agreement with the simple correction model. The slope of the mixing line (error-weighted linear regression slope) yields a ^{232}Th -free $^{230}\text{Th}/^{238}\text{U}$ activity ratio and a $\delta^{234}\text{U}$ of 0.0456 ± 0.0078 and $+210.7 \pm 4.5\text{‰}$, respectively, which correspond to an average age of these three samples of 4200 ± 750 years. The mean of the single ^{232}Th corrected ages is 4350 ± 570 and is thus equal to the isochron result within uncertainty. This result strongly supports our

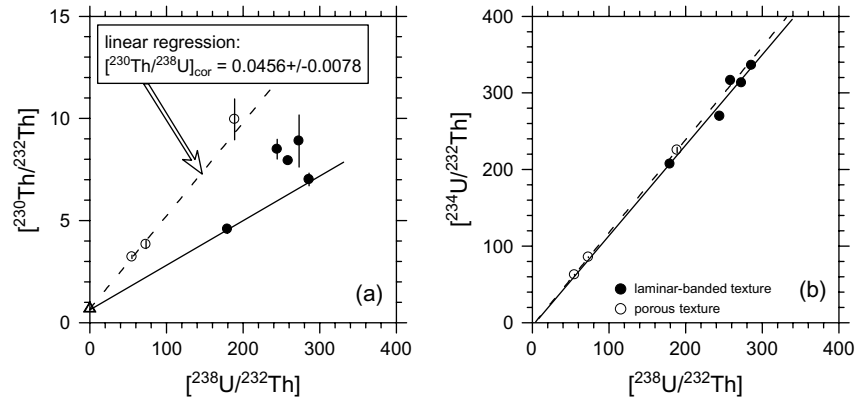


Figure 4 Rosholt Type II isochrons of U series nuclides of sample u15.156: (a) $[^{230}\text{Th}/^{232}\text{Th}]$; (b) $[^{234}\text{U}/^{232}\text{Th}]$. Open symbols represent the three porous layers close to the tunnel wall. Filled symbols represent laminar-banded calcite layers. The dashed line gives an error-weighted linear regression through the open symbols. The black line is simply a straight line through the outermost two samples of youngest age. The open triangle represents the detrital $^{230}\text{Th}/^{232}\text{Th}$ activity ratio used in our simple correction model.

simple model used to correct the influence of detritus on single $^{230}\text{Th}/\text{U}$ ages. In addition, the small value of the intercept of the linear regression line ($[^{230}\text{Th}/^{232}\text{Th}]_0 = 0.64 \pm 0.2$) as well as the intercept of a linear trend line through the youngest two samples (see Fig. 4 (a)) indicate that no ^{230}Th was deposited in excess of detrital U (initial ^{230}Th component) during calcite formation, which could also disturb the age calculation. The intercept of the isochron to determine the ^{232}Th -free $\delta^{234}\text{U}$ (Fig. 4 (b)) is ± 0 within uncertainty of the error-weighted regression line, indicating secular equilibrium of ^{234}U and ^{238}U in the detrital fraction, as expected.

However, each of the studied pieces of calcite overgrowth certainly has its own complex and variable chemical composition. For example, some calcite layers contain minor amounts of fine ash and limestone particles or have remains of organic matter. It is important to note that one would need to study each calcite layer of the other four pieces in more detail (similar to the sample u15.156) to ensure that our correction model holds for all investigated calcite layers. As most of the other samples were significantly younger, or the oldest parts were strongly altered and thus not datable, we skipped further investigation. Also, layers containing ash particles were not analysed, even though it would be interesting to determine the exact date of the use of open fire at the entrance of the tunnel or within it.

The ^{232}Th corrected $^{230}\text{Th}/\text{U}$ ages of single growth bands (see Fig. 3 and Table 1) range from 4600 to 1700 years, clearly indicating that the tunnels had been built during early phases of Troy and were used until Roman times.

Taking all uncertainties into consideration, we conclude that the calcite started to overgrow the tunnel walls earlier than 4000 years ago. Therefore, this part of the tunnel (i.e., the location of samples u15.156; u15.238 and u15.14-19, see Fig. 1) was built during the early phases of the 'Maritime Troy Culture' (= Troy I–II) and maintained during its end phases (Troy III). This period corresponds to the Early Bronze Age at Troy (c. 2900–2250 BCE), to which the famous 'Treasures of Troy' belong (c. 2500 BCE). This is also the time during which this site had an especially important international role. Culturally, it was mainly oriented towards Anatolia and the Near East, but trading links can be assured reaching far into Europe, the Mediterranean and Central Asia. Recent work in the excavation has established the existence of an upper city (or

citadel) and a fortified lower city (Korfmann 1999). When first constructed, the water system would have lain within the defences of the lower city, a fact that underlies its importance at that time. For the inhabitants of Troy in the second millennium BCE, therefore, these subsurface water systems or 'water quarries' were something that was inherited from the remote past. Within the Luwian and Hittite world of the second millennium BCE it would not be surprising, then, if they were regarded as a superior system, and so were identified with the god KASKAL.KUR. This offers some further support for the generally accepted identification of Wilusa/Taruisa with Troy VI–VIIa.

The early date of the water tunnel also lends weight to the idea that the construction of such tunnels was possible long before the general use of iron. Although this in opposition to the general view, a third millennium BCE date for such 'water quarries' is considered a possibility (Grewe 1998).

We found that the artificial tunnels were filled with water until approximately 1700 years ago. This agrees fairly well with archaeological evidence concerning the duration of their use. Between about 2500 and 1700 years ago, open fire had been used in the entrance area or within the tunnels, as recorded by fine ash particles within the youngest calcite layers of samples u.15.14–19 and the centre part of sample u15.132.

REFERENCES

- Baker, A., Smart, P. L., Edwards, R. L., and Richards, D. A., 1993, Annual growth banding in a cave stalagmite, *Nature*, **364**, 518–20.
- Bard, E., Arnold, M., Hamelin, B., Tisnerat-Laborde, N., and Cabioch, G., 1998, Radiocarbon calibration by means of mass spectrometric $^{230}\text{Th}/^{234}\text{U}$ and ^{14}C ages of corals: an updated database including samples from Barbados, Mururoa and Tahiti, *Radiocarbon*, **40**(3), 1085–92.
- Burns, S. J., Matter, A., Frank, N., and Mangini, A., 1998, Speleothem-based paleoclimate record from northern Oman, *Geology*, **26**(6), 499–502.
- Cheng, H., Edwards, R. L., Hoff, J., Gallup, C. D., Richards, D. A., and Asmeron, Y., 2000, The half-lives of uranium-234 and thorium-230, *Chemical Geology*, **169**, 17–33.
- Edwards, R. L., Beck, J. W., Burr, G. S., Donahue, D. J., Chappell, J. M. A., Bloom, A. L., Druffel, E. R. M., and Taylor, F. W., 1993, A large drop in atmospheric $^{14}\text{C}/^{12}\text{C}$ and reduced melting in the younger Dryas, documented with ^{230}Th ages of corals, *Science*, **260**, 262–97.
- Eisenhauer, A., Wasserburg, G. J., Chen, J. H., Bonani, G., Collins, L. B., Zhu, Z. R., and Wyrwoll, K. H., 1992, Holocene sea-level determination relative to the Australian continent: U/Th (TIMS) and ^{14}C (AMS) dating of coral cores from the Abrolhos Islands, *Earth and Planetary Science Letters*, **114**, 529–47.
- Frank, N., Braun, M., Hambach, U., Mangini, A., and Wagner, G., 2000, Warm period growth of travertine during the last interglaciation in southern Germany, *Quaternary Research*, **54**, 38–48.
- Frumkin, A., Ford, D. C., and Schwarcz, H. P., 1999, Continental oxygen isotopic record of the last 170 000 years in Jerusalem, *Quaternary Research*, **51**, 317–27.
- Grewe, K., 1998, *Licht am Ende des Tunnels. Planung und Terrassierung im antiken Tunnelbau*, Verlag Philipp von Zabern, Mainz am Rhein.
- Ivanovich, M., and Harmon, R. S., 1992, *Uranium-series disequilibrium: applications to earth, marine, and environmental sciences*, Clarendon Press, Oxford.
- Kaufman, A., and Broecker, W., 1965, Comparison of Th-230 and C-14 ages for carbonate materials from lakes Lahontan and Bonneville, *Journal of Geophysical Research*, **70**(16), 4039–54.
- Korfmann, M., 1994, Troia: a residential and trading city at the Dardanelles, *5th International Aegean Conference*, 173–83.
- Korfmann, M., 1996, The citadel and lower city of Troia at the Dardanelles. City of war and peace where seas and continent meet, in *Housing and settlement in Anatolia. A historical perspective* (ed. Y. Sey), 83–98, UN Conference Habitat II.
- Korfmann, M., 1998a, Troia, an ancient Anatolian palatial and trading center, *The Classical World*, **91**(5), 369–85.
- Korfmann, M., 1998b, Troia—Ausgrabungen 1997, *Studia Troica*, **8**, 1–70.

- Korfmann, M., 1999, Troia—Ausgrabungen 1998, *Studia Troica*, **9**, 1–34.
- Korfmann, M., 2000, Homers Troia: Griechischer Aussenposten oder hethitischer Vasall? *Spektrum der Wissenschaften*, July, 64–70.
- Ludwig, K. R., and Titterton, D. M., 1994, Calculation of $^{230}\text{Th}/\text{U}$ isochrons, ages, and errors, *Geochimica et Cosmochimica Acta*, **58**(22), 5031–42.
- Neff, U., Burns, S. J., Mangini, A., Mudelsee, M., Fleitmann, D., and Matter, A., 2001, Strong coherence between solar variability and the monsoon in Oman between 9 and 6 kyr ago, *Nature*, **411**, 290–2.
- Starke, F., 1997, Troia im Kontext des historisch–politischen Umfeldes Kleinasien im 2. Jahrtausend, *Studia Troica*, **7**, 447–87.
- Sturchio, N. C., Pierce, K. L., Murrell, M. T., and Sorey, M. L., 1994, Uranium-series ages of travertine and timing of the last glaciation in the Northern Yellowstone Area, Wyoming–Montana, *Quaternary Research*, **41**, 265–77.
- Wedepohl, K. H., 1995, The composition of the continental crust, *Geochimica et Cosmochimica Acta*, **59**(7), 1217–32.
- Williams, P. W., Marshall, A., Ford, D. C., and Jenkinson, A. V., 1999, Palaeoclimatic interpretation of stable isotope data from Holocene speleothems of the Waitomo district, North Island, New Zealand, *The Holocene*, **9**(6), 649–57.

